Available online at www.sciencedirect.com
SCIENCE DIRECT®
Journal of Photochemistry and Photobiology A: Chemistry 161 (2003) 27–34
Journal of Photochemistry and Photobiology A:Chemistry
www.elsevier.com/locate/jphotochem

Antibacterial textiles prepared by RF-plasma and vacuum-UV mediated deposition of silver

T. Yuranova [a], A.G. Rincon [b], A. Bozzi [a], S. Parra [a], C. Pulgarin [b], P. Albers [c], J. Kiwi [a,*]

[a] *Laboratory of Photonics and Interfaces, Institute of Molecular Chemistry and Biology, EPFL, Lausanne 1015, Switzerland*
[b] *Laboratory of Biological Engineering, ENAC EPFL, 1015 Lausanne, Switzerland*
[c] *Degussa AG, Ind Wolfgang, Rodenbacher Chaussee 4, Hanau/Main, Germany*

Received 9 April 2003; accepted 22 April 2003

Abstract

The bacterial inactivation efficiencies of silver metal and oxides and their combinations on textile fabrics was investigated to evaluate the disinfectant action on airborne bacteria. The inactivation performance was seen to depend on the amount of silver on the textile surface. The preparation of the polyester–polyamide Ag-loaded textiles was carried out by RF-plasma and vacuum-UV (V-UV) surface activation followed by chemical reduction of silver salts. The rate of bacterial inactivation by the silver loaded textile was tested on *Escherichia coli* K-12 and showed long lasting residual effect. Specular reflectance has been employed to assess the optical properties of the Ag-loaded fabrics. By elemental analysis it was found that levels of Ag loading >0.118% (w/w) for the vacuum-UV samples lead to complete inhibition of bacterial growth. X-ray photoelectron spectroscopy (XPS) shows that for textiles activated by RF or V-UV methods, the silver in the topmost layer increases with increasing concentration of the Ag used in the precursor solution. The exact determination of the oxidation state of the Ag-clusters on the textile is difficult because of the variation of particle size and electrostatic charging of the supported particles. Ag metal was found to be the main component of the Ag-clusters and not Ag_2O and AgO as identified by the binding peak energies (BE). By transmission electron spectroscopy (TEM) it was seen that the Ag-clusters were deposited on the two polymer components of the textile fabric but having widely different sizes.

Keywords: Antibacterial textiles; Biological testing; Ag deposition; RF-plasma; Vacuum-UV; XPS of Ag-clusters; Size of Ag-clusters

1. Introduction

Silver has been known as a disinfectant for many years and is being used in many forms in the treatment of infectious diseases [1–3] and has a broad spectrum antibacterial activity while exhibiting low toxicity towards mammalian cells. In a very low concentration silver-ions are effective against bacteria in water systems [4,5]. The mechanism of silver antibacterial action is poorly understood. Three mechanisms for the latter effect have been proposed: (a) interference with bacterial electron transport; (b) binding to the bacterial DNA after in low concentration Ag enters the cell. As a reaction against the denaturation effect of Ag/Ag-ions, DNA condenses loosing their replication ability [6] or interacts with protein thiol groups inactivating the latter; and (c) interaction with cell wall membrane without entering the cell forming reversible sulfhydryl or histidyl complexes on the cell surface and preventing dehydro-oxygenation process [7–9].

This investigation is directed towards the fixation and catalytic performance of Ag-clusters on polyamide–polystyrene textile fabrics. After a long series of preliminary experiments, the most suitable experimental conditions for the RF-plasma and vacuum-UV (V-UV) activation of the fabric surface were found. Then the chemical deposition of Ag-clusters was carried out on these activated surfaces checking subsequently each Ag deposit against the antibacterial activity observed. Once the optimization of the Ag-clusters was completed the latter clusters were characterized by complementary surface techniques like: diffuse surface reflectance (DRS), elemental analysis, X-ray photo-electron spectroscopy (XPS), and transmission electron microscopy (TEM).

* Corresponding author. Fax: +41-21-693-4111.
E-mail address: john.kiwi@epfl.ch (J. Kiwi).

1010-6030/$ – see front matter © 2003 Elsevier Science B.V. All rights reserved.
doi:10.1016/S1010-6030(03)00204-1

2. Experimental

2.1. Materials

Reagents like $AgNO_3$, ammonia, isopropanol, Ag_2CO_3 were Fluka p.a. and used without further purification. Deionized water was employed throughout this work.

2.2. Functionalization of textile fabrics by RF-plasma

The textile polymer fabric surface was treated in a RF-plasma cavity (Harrick Corp., 13.56 MHz, 100 W) at a pressure of 0.8 Torr. A variety of oxygen functional groups: >C–O, >C=O,–O–C=O, –COH, –COOH were produced on the fabric through the reaction between the active species induced by the plasma in the gas phase and the C-surface atoms [10]. Besides the functional groups mentioned previously, synthetic textiles have been shown to form a significant number of carboxylate, per-carboxylate, epoxide and peroxide groups upon irradiation with RF-plasma [2–5]. These oxygen functionalities obtained by oxygen plasma are located in the topmost layers and increase with longer treatment time, but remain constant with treatment time >30 min. This is why the latter time has been chosen for RF-plasma treatment.

2.3. Functionalization of textile fabrics by vacuum-UV

The textile polymer surface was also functionalized by vacuum-UV irradiation using the 185 nm line from a 25 W low pressure mercury lamp (Ebara Corp., Tokyo, Japan). The lamp tube is synthetic silica tube. Lower energies than RF-plasma are attained by vacuum-UV activation. The oxygen gas (0.8 Torr) in the plasma cavity forms only excited states or is converted to atomic species.

Table 1
Percentage surface composition of RF-plasma loaded silver textiles

	0.05 g/200 ml $AgNO_3$ solution	0.3 g/200 ml $AgNO_3$ solution	1 g/200 ml $AgNO_3$ solution
C 1s	63.2	63.3	69.7
N 1s	1.13	0.82	0.92
O 1s	33.0	33.6	26.7
Na 1s	–	–	0.59
Si 2p	2.70	1.85	1.45
Cl 2p	–	–	
Ag $3d_{5/2}$	0.06	0.40	0.62

2.4. Loading of silver on activated textile fabrics

After functionalizing the textile surfaces by RF-plasma or vacuum-UV the fabrics are immersed in solutions with different concentrations of $AgNO_3$ as noted in Tables 1 and 2. Afterwards the silver is reduced at a suitable pH with mild reducing agent [11] and the final fabric presenting a dark yellow color is dried in air at room temperature.

2.5. Bacterial growth testing

Textiles with silver attached and textiles without silver that have not been previously sterilized are incubated for 24 h at 37 °C in Luria Bertani media (LB) plates under controlled conditions. After the latter time period the assessment of partial or total bacterial inhibition by the Ag-loaded fabric is observed and compared with the non-loaded fabric. To determine bacterial survival in water, *Escherichia coli* K-12 was used as a bacterial model. Cultures in the exponential phase of growth were obtained using an aliquot part of the inoculum grown overnight in 20 ml of Luria Bertani media at 37 °C. After centrifugation, the cells were re-suspended in tryptone (Merck AG) solution. Finally, the cell suspensions were diluted with Milli-Q deionized water to the required cell density corresponding to 10^4 colony forming units (CFU)/ml.

In a typical experiment, bacterial suspensions were contacted with the textile fabric for 24 h in the dark and samples were plated on agar PCA (plate count Agar, Merck AG, Germany). The plates were incubated at 37 °C for 24 h before counting and the reported results were the media of three experimental runs.

Additional tests were carried out using *Pseudomonas aeruginosa* following Swiss EMPA Norms 2003 and for *Bacillus subtilis* and *Aspergillus niger* according to Swiss EMPA Norms 510. The bacterial growth inhibition followed the same pattern as observed for the case of *E. coli* K-12.

Table 2
Percentage surface composition of vacuum-UV loaded silver textiles

	0.1 g/200 ml $AgNO_3$ solution	0.3 g/200 ml $AgNO_3$ solution	0.5 g/200 ml $AgNO_3$ solution	0.7 g/200 ml $AgNO_3$ solution	0.9 g/200 ml $AgNO_3$ solution
C 1s	73.9	70.8	70.6	68.1	73.3
N 1s	2.9	3.2	3.7	2.8	2.6
O 1s	21.9	23.9	22.1	24.3	20.7
Na 1s	0.33	–	–	–	–
Si 2p	0.70	1.25	1.44	2.27	1.51
S 2p	0.08	0.2	0.34	0.37	0.33
Cl 2p	0.06	0.06	0.10	0.13	0.08
Ag $3d_{5/2}$	0.25	0.64	1.57	2.02	1.87

2.6. Diffuse reflectance spectroscopy

These measurements have been carried out in a Cary-5 spectrophotometer equipped with an integrating sphere. The base line used was relative to the response of the instrument to a calibrated sample of $MgCO_3$.

2.7. Elemental analysis

Elemental analysis of the Ag loading on the textile fabrics was carried out in a Perkin-Elmer unit 300 s.

2.8. X-ray electron spectroscopy (XPS)

Measurements were carried out in a Leybold-Heraeus instrument calibrating the binding energies (BE) to the Au $f_{7/2}$ level taken as 84.0 eV. The evaluation of the binding energies of the Ag-clusters was carried out following the DIN norms [12] and after taking into consideration the sensitivity factors allowed a reproducibility of ±5% in the measurements. The spectra were analyzed in a DS 100 data set after X-ray satellite subtraction and smoothing of the polynomial fit. The relative sensitivity factors used were: O 1s 0.78; C 1s 0.78; S 2p 0.84; Ag $3d_{5/2}$ 3.23. The quantitative evaluation of the experimental data was carried out with a Shirley type background correction due to the electrostatic charging of the particles during the measurements [13]. Electrostatic charging effects were referenced calibrating to the C 1s signal.

2.9. Transmission electron microscopy (TEM)

Electron microscopy was carried out with a the Philips CM 120 microscope to observe the Ag-clusters on the textile surface. The instrument used for electron microscopy (120 kV, 0.35 nm point resolution) was equipped with energy dispersive X-ray analysis (EDXA) to identify the deposition of Ag-clusters on the textile fabric.

3. Results and discussion

3.1. Biological testing of the Ag-loaded textile prepared by RF-plasma activation

Fig. 1(a) shows the effect of Ag-loaded textiles surfaces activated by RF-plasma on the airborne bacteria after 24 h. The antibacterial effect reported in Fig. 1(a) was carried out in the dark. Adsorption of bacteria on the textile was observed on the unloaded fabric and as well as on the Ag-loaded fabric. The abscissa refers to the $AgNO_3$ grams in 200 ml solution used in the silver loading after the RF-plasma treatment. After the relative index of 0.3 g $AgNO_3$/200 ml solution (Fig. 1 trace (A)), the inhibition of bacterial activity at 24 h seems to be complete. This suggests that a direct contact between the bacteria and the textile having an adequate density of silver clusters is necessary for the bacterial abatement process to proceed. The latter observation is consistent with some recent work on the mechanism of bacterial abatement due to metal/oxides and ions [1,2,6]. Lower levels of silver loading in the textile do not allow the formation of a sufficient number of Ag-clusters necessary for the total inhibition of bacterial growth.

Fig. 1(b) shows the decrease in the number of *E. coli* K-12 colonies suspended in Milli-Q water as a function of time in contact with a textile sample activated by RF-plasma with ($AgNO_3$ solution, 1 g/200 ml) and for a second control fabric without silver loading. It is readily seen from Fig. 1(b), that during 24 h the Ag-loaded fabric inhibits any bacterial growth. Moreover, a bacterial decrease from 10^4 CFU/ml to a non-detectable level below 10 CFU/ml was detected within 24 h. The control fabric shows only a modest reduction of one order of magnitude due to adsorption of *E. coli* K-12 on the textile fabric surface.

3.2. Biological testing of the Ag-loaded textile prepared by vacuum-UV activation

Fig. 2(a) shows total inhibition of airborne bacterial activity at concentrations ≥0.5 g $AgNO_3$/200 ml solution. The latter concentration of silver is seen to be slightly higher than the value needed for completed bacterial inhibition reported in Fig. 1(a). This reveals that the density active sites—whatever their nature—is different in the vacuum-UV activated sample than in the RF-Plasma treated sample. A slightly higher amount of silver seems to attach to the active sites on the textile in vacuum-UV treated sample and this will be discussed below in the section related to elemental analysis of Ag on the textile fabrics. The action of the 185 nm (6 W) component of the 254 nm mercury light used produces excited states of oxygen, atomic oxygen and non-ionic gaseous radicals since there is not enough energy to create ionic oxygenated species as it is the case of RF-plasma [10]. These gaseous oxygen activated species interact with the textile and would increase the peroxide surface radicals besides the carboxy and percarboxylic radical species. These radicals in the presence of air water vapor hydrolyze to form carboxylic, percarboxylic acid terminals as well as $OH^{\bullet}$ and $HO_2^{\bullet}$ on the textile surface which are able to chelate silver-ion. A similar procedure is used to fix Al-ions on styrene polymer surface by way of vacuum-UV surface treatment [14].

Fig. 2(b) shows the decrease in the number of *E. coli* K-12 colonies as a function of contact time for a control textile fabric without silver loading and for the vacuum-UV pretreated fabric loaded with $AgNO_3$ solution (1 g/200 ml). After 30 min the concentration of *E. coli* K-12 had been reduced below the detectable level (<10 CFU/ml). It is readily seen from Fig. 2(b), that the latter effect due to the Ag-loaded fabric has the character of a lasting inhibitory effect up to 24 h. The control fabric shows a modest reduction of the number of initial bacteria on the fabric surface due to bacterial adsorption on the textile surface.

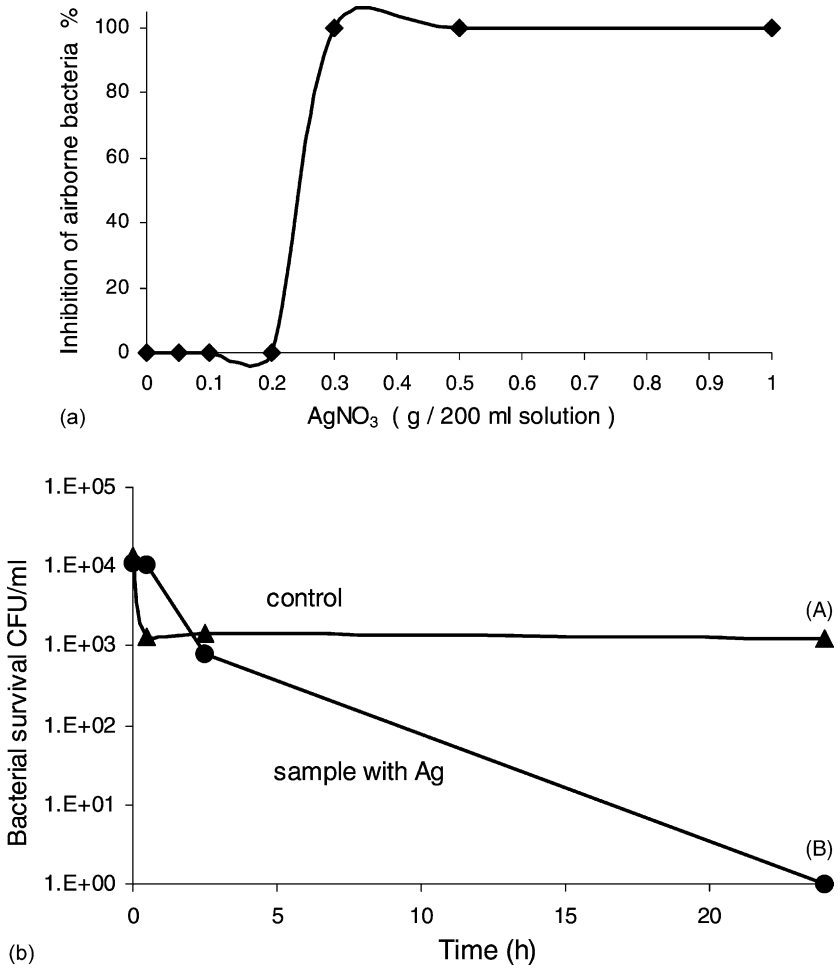

Fig. 1. (a) Inhibition of airborne bacterial growth by textile fabrics activated by RF-plasma as a function of the textile Ag loading. (b) Bacterial survival (CFU/ml) of an RF-plasma activated textile surface as a function of time for: (A) control textile and (B) textile loaded with an $AgNO_3$ sample solution (1 g/200 ml).

3.3. Diffuse reflection spectroscopy of silver loaded textiles pretreated by vacuum-UV

Fig. 3 shows the specular reflectance for the textile fabrics activated by vacuum-UV loaded with a different amount of silver. The textiles turn from white to yellow-beige colored materials with decreasing specular reflection as the silver concentration used in the preparation of the samples goes up due to the increased optical absorption (coloration) of the sample. This is a direct measure that the Ag abundance in the topmost layer of the textile fabric used. The continuous close profile of the curves presented in Fig. 3 for the different Ag loadings shows a similar receptivity of the surface for the Ag-clusters of different sizes.

3.4. X-ray photoelectron spectroscopy (XPS) of RF-plasma and vacuum-UV activated surfaces loaded with silver

The percentage surface composition of RF-plasma loaded silver textiles by XPS spectroscopy is presented in Table 1. The silver content of topmost layer surface of the textile increases with the concentration of the silver solution used to react this metal with the functional groups introduced on the textile by RF-plasma. The reference for the values obtained has been carried out according to reference [13] comparing the spectra obtained with related spectra of silver found in the scientific literature. The background correction for the obtained signals was carried out according to [12]. The values reported in Table 1 do not represent bulk or deeper layer content of silver that can be treated as integral value for the attached silver. This observation will be discussed with the right perspective in relation to the Ag found by elemental analysis in the last section below.

The binding energies (BE) of the silver were quantified for the silver species deposited on the textiles for the different concentrations of silver used. For 0.05, 0.3 and 1 g $AgNO_3$/200 ml solution, the BE was close to 368.2 eV which is the reference value for metallic Ag [15]. The reference values for the BE of Ag_2O was 367.8 eV and AgO 367.4 eV.

Table 2 presents the percentage surface composition for vacuum-UV activated silver textiles. Table 2 shows a

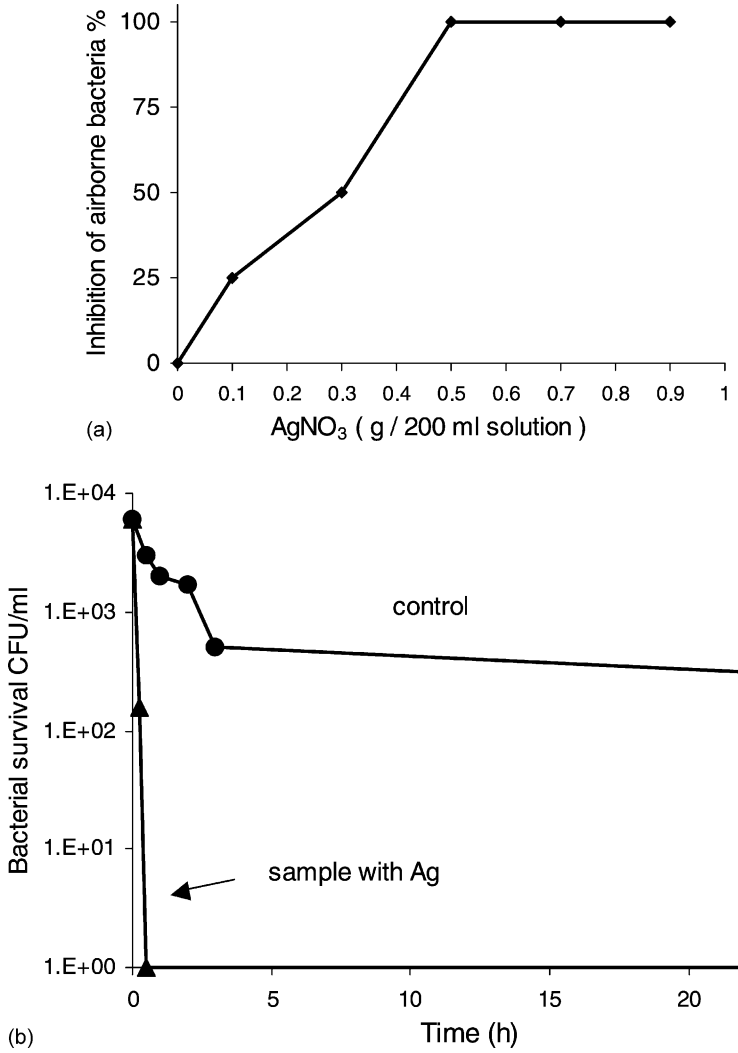

Fig. 2. (a) Inhibition of airborne bacterial growth by textile fabrics activated vacuum-UV as a function of the textile Ag loading. (b) Bacterial survival (CFU/ml) of a vacuum-UV activated textile surface as a function of time for: (A) control textile and (B) textile loaded by using an $AgNO_3$ sample solution (1 g/200 ml).

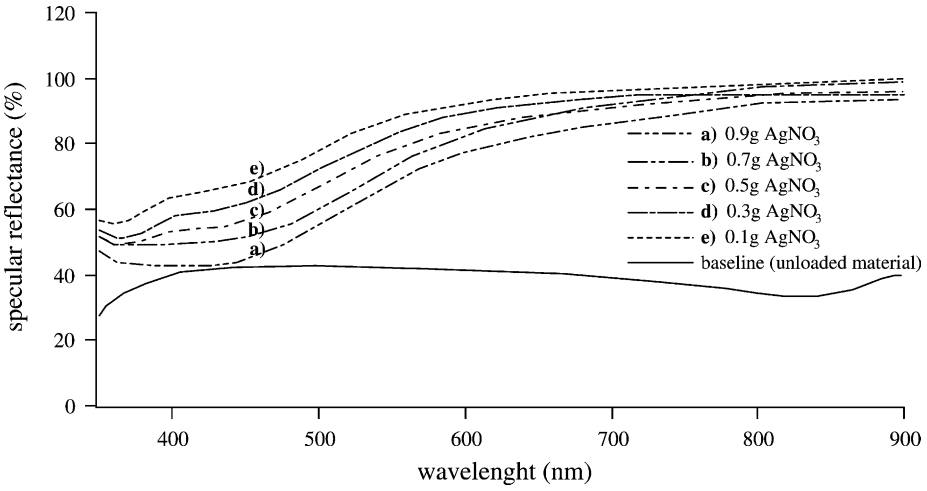

Fig. 3. Percentage specular reflectance for textile surfaces loaded with different concentrations of Ag. For other details see caption in this figure.

systematic increase for the Ag present in the topmost atomic layer with the concentration of silver used in the loading of the textile surface. For the 0.9 g $AgNO_3$/200 ml sample a small decrease in the Ag concentration compared to the 0.7 g $AgNO_3$/200 ml sample was observed due to the presence of some large surface silver particles. A higher concentration of silver leads to a significant particle growth on the textile surface as observed by TEM. The XPS signal intensities are influenced by the Ag surface concentration as well as by the dispersion and size of the Ag on the textile surface. The exact determination of the silver surface abundance is difficult because of the variation in particle sizes (see Section 3.5 below on electron microscopy) and the electrostatic effects on the textile supported Ag-clusters.

The binding energies (BE) of the silver clusters were also quantified for the silver species deposited on the textiles for the different concentrations of silver used. For a sample prepared with 0.1 g $AgNO_3$/200 ml solution, the BE observed was close to 367.8 eV which is the reference value for Ag_2O [15]. The latter cluster consisted mostly of Ag_2O with a minor component of AgO (367.4 eV). But, for all the other Ag concentrations as shown in Table 2, the BE were close to 368.2 eV indicating almost total metallic Ag-clusters.

3.5. Transmission electron microscopy (TEM) of Ag-loaded fabrics activated by RF-plasma and vacuum-UV

Fig. 4(a) shows the TEM of the thick polyamide fiber component of the textile fabric loaded with 0.3 g $AgNO_3$/200 ml solution after RF-plasma activation. The latter loading of silver on the fabric corresponds to the minimum loading necessary for complete inhibition of bacterial growth as shown previously in Fig. 1(a). The size of the Ag-clusters varied between 50 and 500 nm. The spacing between the fibers was observed to be highly irregular. The heterogeneous deposition of the Ag-clusters on the textiles is probably due to the numerous oxygen gas species produced during RF-plasma leading subsequently to different anchoring groups on the textile surface. Fig. 4(b) shows Ag-clusters on thinner poylester fibers with a more regular spacing on the fiber surface. The size of the clusters was seen also to vary widely between 8 and 40 nm counting around 100 Ag-clusters.

Fig. 5(a) presents the Ag-clusters prepared with a 0.5 g $AgNO_3$/200 ml solution applied on the fabric that was previously activated by vacuum-UV. This is minimum loading necessary for complete inhibition of bacterial growth as shown in Fig. 2(a). The size of the Ag-clusters was seen to vary between 4 and 6 nm for the polyamide component and the shape of the clusters was almost entirely spherical with a few dendritic structures. The space between the Ag-clusters was seen to be much more regular than when the fabric was pretreated with RF-plasma. This becomes understandable in terms of the vacuum-UV species in the gas phase of the irradiation set-up leading only to lower energy species like excited oxygen and atomic oxygen. The latter species are much more homogeneous in the number of single species available to the gas phase than the more complex higher energy ionized species produced in the gas phase by RF-plasma [10,14]. Fig. 5(b) presents the Ag-clusters on the textiles with a mean diameter of 6 nm for textiles loaded with 1.0 g $AgNO_3$/200 ml solution. The regular distribution of the clusters on the support is due to the vacuum-UV activation and is readily noticed in Fig. 5(b).

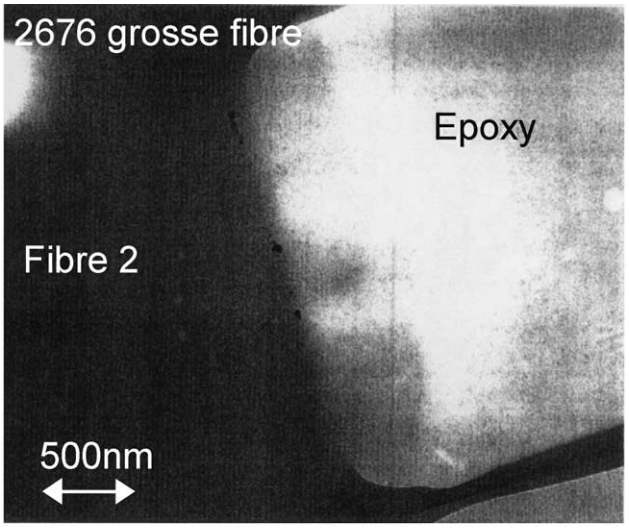

(a)

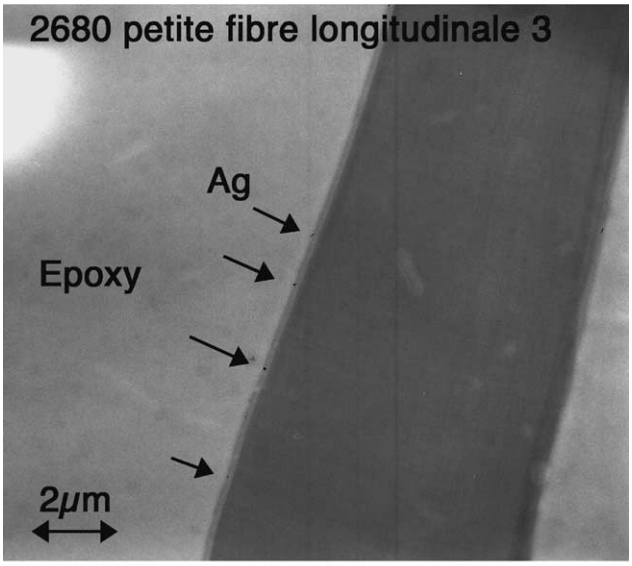

(b)

Fig. 4. (a) Transmission electron microscopy of Ag-clusters on the thick polyamide fiber component of the textile fabric. Activation of the fabric by RF-plasma. (b) Transmission electron microscopy of Ag-clusters on the thin polyester fiber component of the textile fabric. Activation of the fabric by RF-plasma.

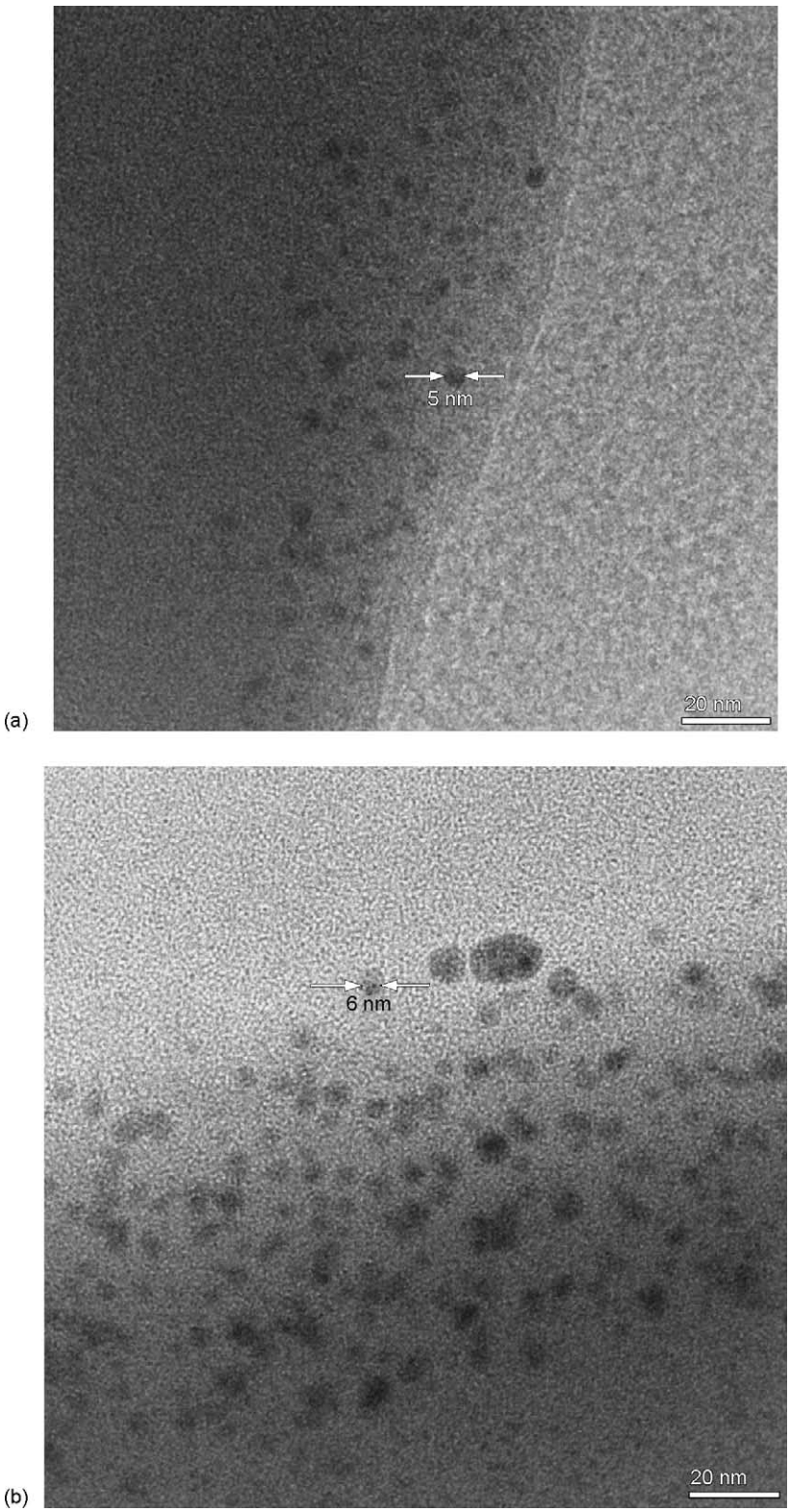

Fig. 5. (a) Transmission electron microscopy of Ag-clusters from a 0.5 g/200 ml $AgNO_3$ solution on the thick polyamide fiber component of the textile fabric. Activation of the fabric by vacuum-UV. (b) Transmission electron microscopy of Ag-clusters from an 1.0 g/200 ml $AgNO_3$ solution on the thick polyamide fiber component of the textile fabric. Activation of the fabric by vacuum-UV.

3.6. Elemental analysis of the Ag-loaded fabrics activated by vacuum-UV

For the five Ag-loaded fabrics presented in Table 2 elemental analysis was carried out to determine the weight of silver per unit size of textile fabric. The results obtained show a very modest increase in Ag weight with increase in the silver concentration used to prepare the particular fabric. For Ag solutions with 0.1; 0.3; 0.5; 0.7 and 0.8 g $AgNO_3$/200 ml solution, the respective increase in percentage weight of Ag on the fabric was: 0.111; 0.118; 0.122; 0.127, and 0.135%. This data seems in variance with the percentage of surface Ag shown in Table 2 for the same materials. The explanation resides in the fact that by XPS (Table 2a) the enrichment in Ag-clusters in the topmost layer is only detected. But, UV 184 nm light penetrates within several monolayers into the fabric. The penetration depends on the material molecular absorption coefficient, the mobility of the polymer fiber chain under light. When the $AgNO_3$ solution is applied, diffusion will take place inside the fabric layer carrying the Ag atoms to a variable depth inside the fabric. The UV light will also affect the degree of crosslinking of the polyamide and polyester fiber component of the fabric complicating the Ag-cluster distribution on the textile. This latter effect will be accompanied by photo-degradation and complicated by the photo-crosslinking of the fibers occurring during the photo-oxidative coupling reaction between Ag and the functional groups introduced on the textile surface by vacuum-UV.

4. Conclusions

This study has shown the beneficial antibacterial activity of silver grafted on textile fabrics by RF-plasma and vacuum-UV followed by chemical treatment of the silver salt on the fabric surface. A minimum loading of silver was seen to be necessary to inhibit the airborne bacterial growth depending on the method used to activate the textile surface. This effect was also investigated and reported for aqueous suspensions of *E. coli* K-12 taken as a bacterial model. The electron microscopy carried out shows different clusters of silver in size and distribution depending on the type of surface activation of the textile surface. By XPS spectroscopy the silver enrichment of the topmost layer of the fabric was determined as a function of the initial concentration of Ag-salt. An increase was observed in the amount of Ag-clusters as the concentration of the Ag-salt used during the preparation is increased. Data obtained from elemental analysis of the silver per unit surface of fabric reveals a similar silver loading for vacuum-UV samples independently of the concentration of silver salt employed during their preparation. This allows the conclusion that silver diffuses to the inner layers of the fabric by the preparation methods used during his work.

Acknowledgements

The financial support of KTI/CTI TOP NANO 21 (Bern, Switzerland) under Grant no. 5601.1 TNS is appreciated.

References

[1] G. Zhao, E. Stevens, Biometals 11 (1998) 27.
[2] F. Fu-Ren, A. Bard, J. Phys. Chem. B. 106 (2002) 279.
[3] R. Demling, L. deSanti, Wounds 13 (2001) 11.
[4] J. Kusnestov, N. Elomaa, P. Martikainen, Water Res. 35 (2001) 4127.
[5] J. Keheler, J. Bashant, L. Johnson, Y. Li, World J. Microbiol. Biotechol. 18 (2002) 133.
[6] Q. Feng, J. Biomed. Mater. Res. 52 (2000) 668.
[7] H. Klasen, Burns 26 (2000) 131.
[8] R. Tilton, B. Rosenberg, Appl. Environ. Microb. 33 (1978) 1116.
[9] M. Tumer, H. Keksol, S. Devin, Transition Met. Chem. 24 (1999) 13.
[10] C. Chan, T. Ko, H. Hiroaka, Surf. Sci. Rep. 24 (1996) 1–54.
[11] H. Hada, A. Yoshida, A. Kurakake, J. Phys. Chem. 80 (1976) 2728.
[12] DIN Norms N39, National Physics Laboratory, Teddington, UK, 1982.
[13] A. Shirley, Phys. Rev. B5 (1979) 4709.
[14] H. Hiroaka, Microelectron. Eng. 6 (1987) 407.
[15] C. Wagner, W. Riggs, L. Davis, J. Moulder, G. Mullenberg (Eds.), Handbook of X-ray Photo-Electron Spectroscopy, Perkin-Elmer Corp., Eden Prairie, MN 55344, USA.